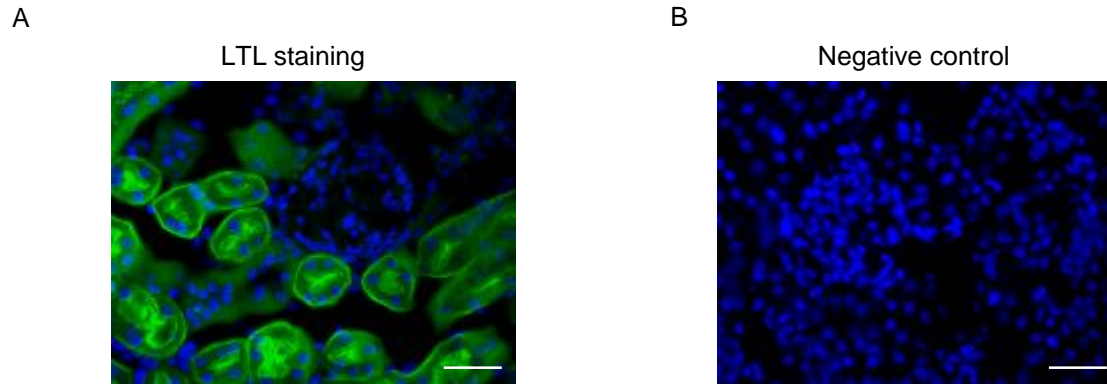


sFigure 1: Detection of L-fucose in normal mouse renal cortex using the plant lectin LTL

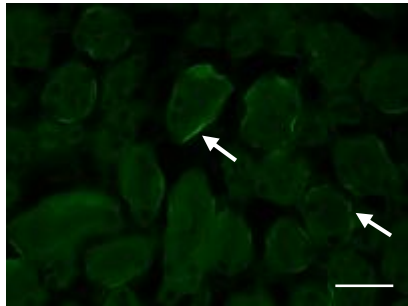


Fluorescence microscopy of normal (*CL-11^{+/+}*) mouse renal tissue after staining with fluorescein-conjugated plant lectin LTL. (a) Positive staining for L-fucose is seen on renal cortical tubules (green), with nuclei stained by DAPI (blue). Scale bars, 250 μm . (b) Similar section but treated with LTL blocked by pre-incubation with L-fucose, confirming the specificity of LTL for detecting L-fucose. Scale bars, 25 μm . The pattern of staining of healthy tubules in this region indicates discrete expression of L-fucose at the apical and basal surfaces of renal tubule cells and weaker more diffuse cytoplasmic expression.

sFigure 2: Baseline C3d in normal CL-11 ^{+/+} kidney (optimal)

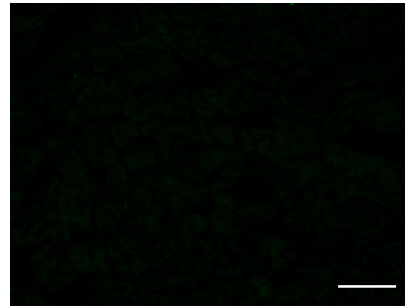
A

C3d staining



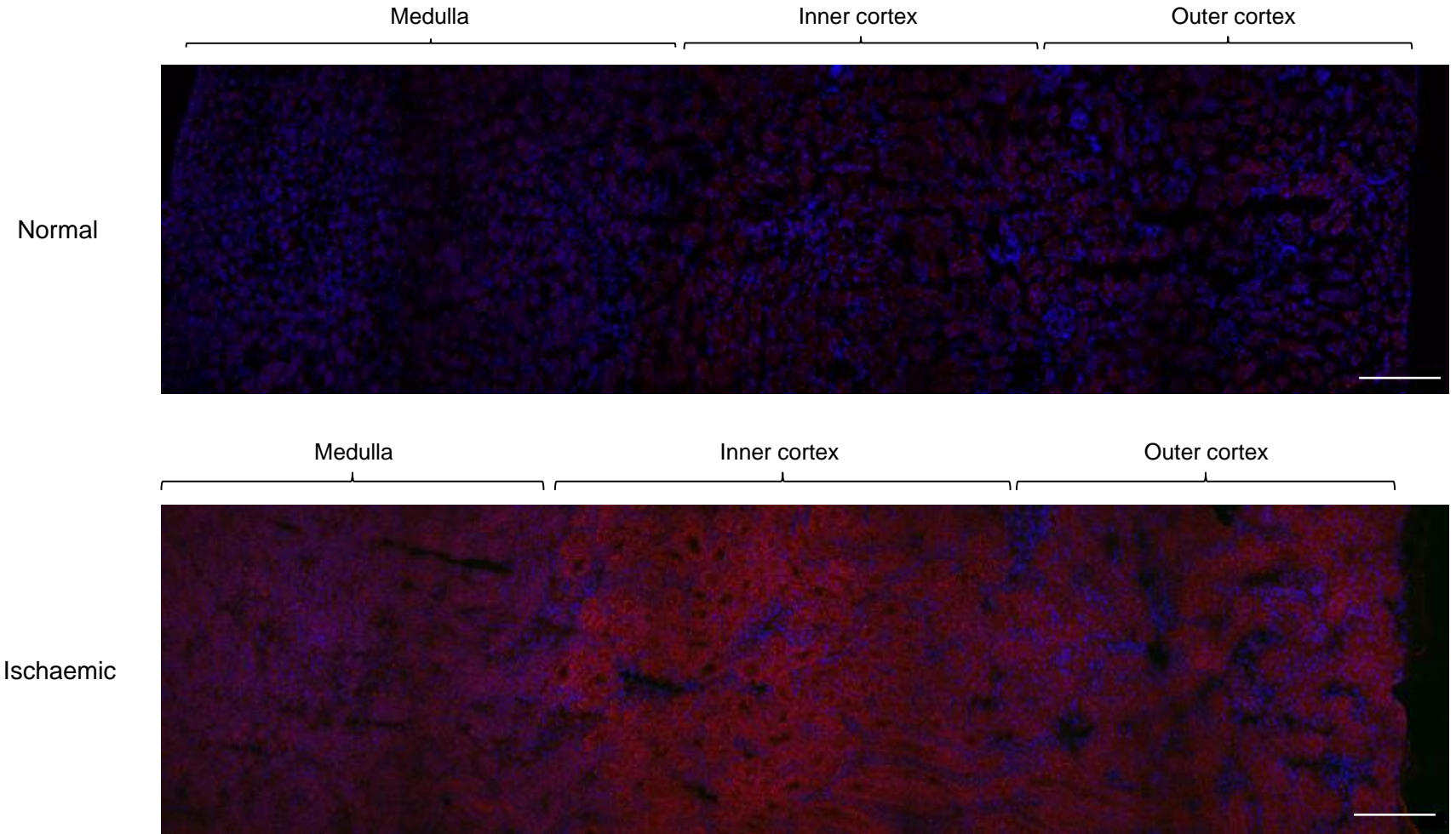
B

Negative control



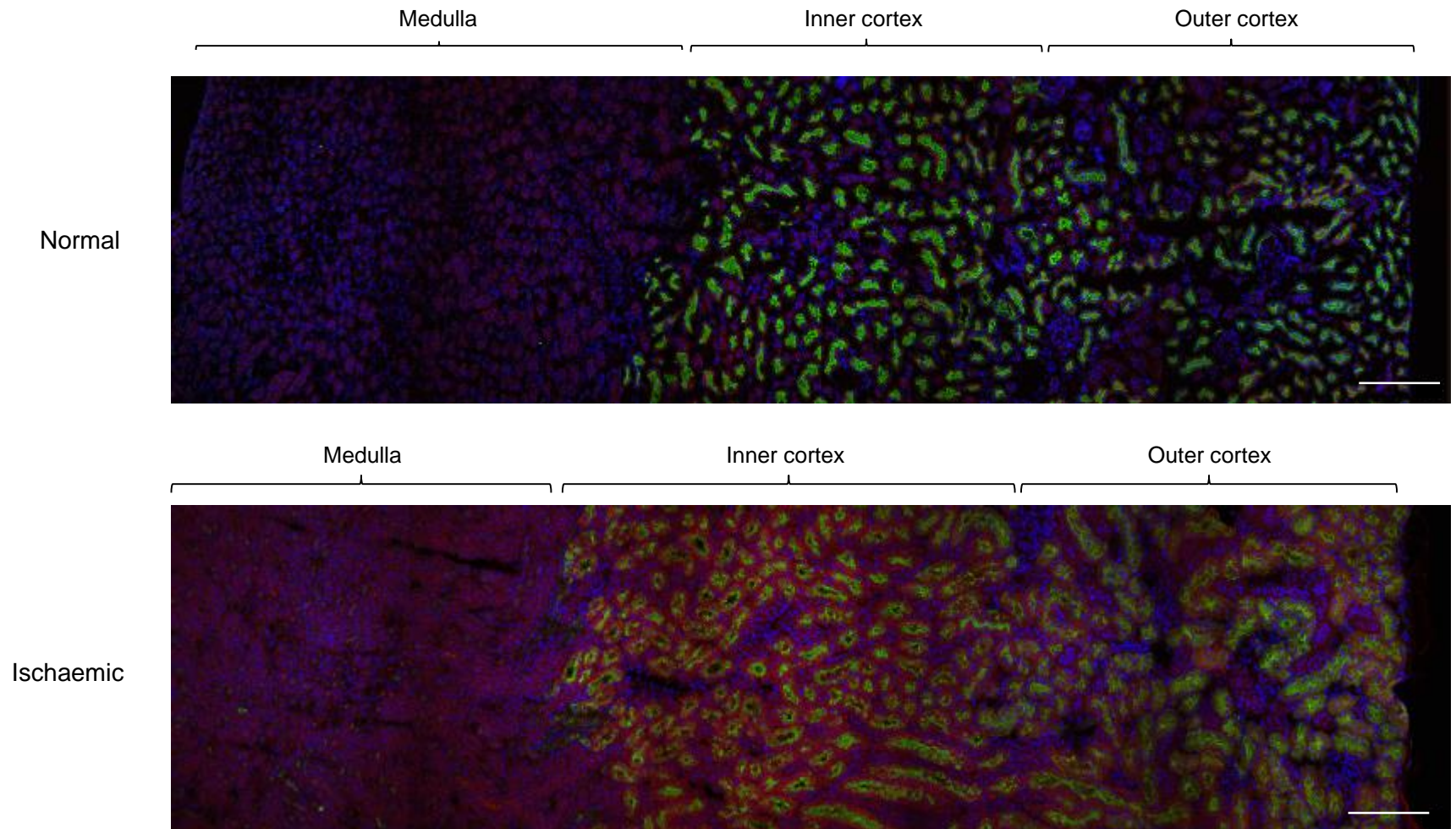
Immunofluorescence microscopy showing C3d in kidney tissue of normal *CL-11^{+/+}* mouse. Kidney tissues were stained with C3d (panel a) or the secondary antibody alone (panel b), demonstrating a basal level of C3d in normal kidney tissue. Arrows indicate the positive stained sites on renal tubules. Scale bars, 25 μ m.

sFigure 3: CL-11 profile in normal and post-ischaemic mouse kidneys



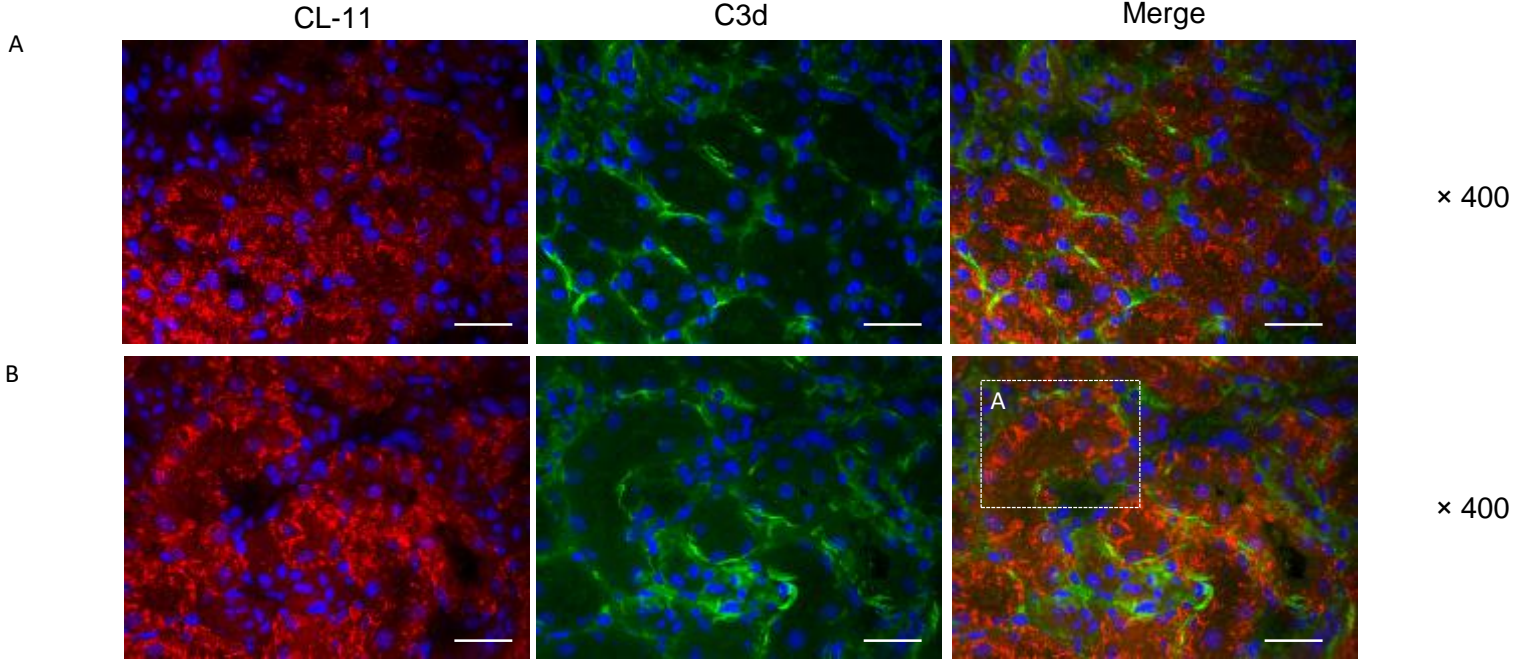
Fluorescence microscopy of *CL-11^{+/+}* mouse kidney showing specific detection of CL-11 (red) and counterstaining of nuclei with DAPI (blue). Broad distribution of CL-11 is seen in normal kidney (upper panel). Increased expression of CL-11 occurs after ischaemia for 30 min and reperfusion for 30 minutes, and is predominant in the tubules of the inner cortex (lower panel). Scale bars, 250 μm .

sFigure 4: L-fucose/CL-11 profiles in normal and post-ischaemic mouse kidneys

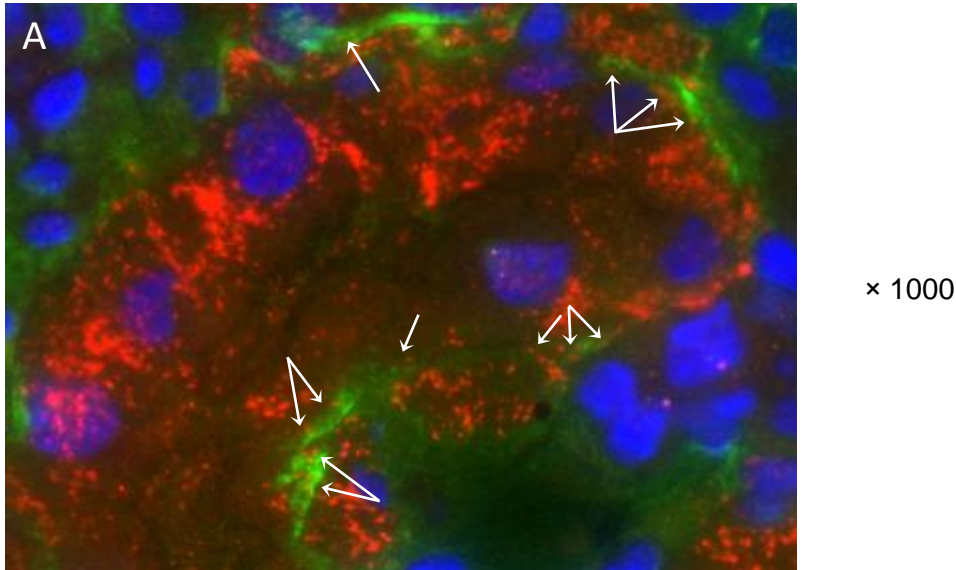


Staining of L-fucose by LTL (green) superimposed on the images obtained for CL-11 (red) and nuclear (blue) staining shown in sFigure 2. The distribution of L-fucose in normal and ischaemic tissue is shown to be restricted to the cortical tubules, where co-expression with CL-11 is particularly evident following the minimum level of ischaemia-reperfusion insult used in this study. Scale bars, 250 μ m.

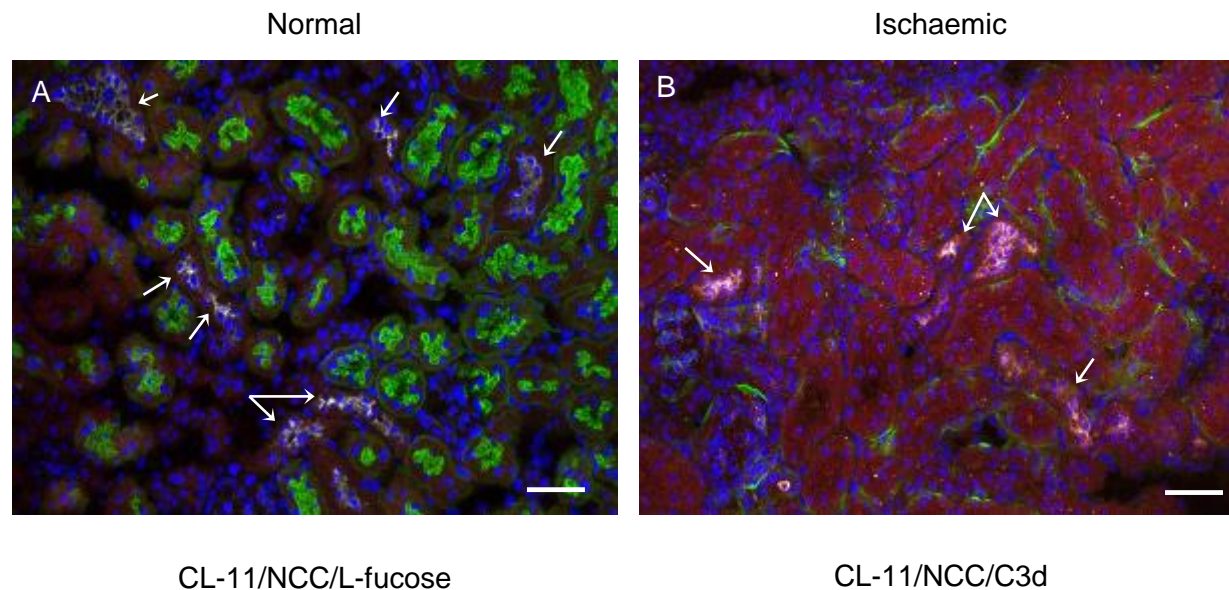
sFigure 5: Localisation of CL-11 and C3d in renal cortex after minimal ischaemia (30 min) and reperfusion (30 min)



Two different sections of post-ischaemic renal tissue showing a mottled pattern of CL-11 detected predominantly at the basolateral border of cortical tubules, seen in cross-section (row A) and also in longitudinal section (row B and magnified image of A). The linear deposits of C3d (green) along the basolateral tubular epithelial border are dotted with CL-11 (orange). Scale bars, 25 μ m.



sFigure 6: CL-11, NCC, L-fucose and C3d profile in mouse kidney



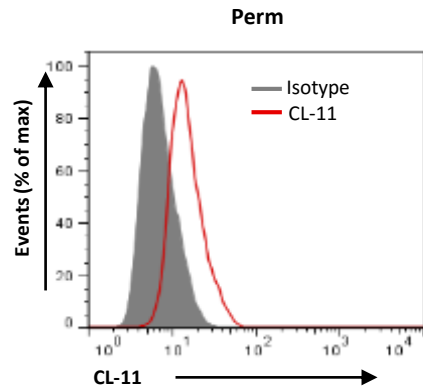
Confocal microscopy with segment-specific markers that distinguish the proximal tubule (L-fucose) and distal tubule (thiazide-sensitive NaCl Co-transporter, NCC) to more precisely map the expression of CL-11 and C3d. (A) Image of normal kidney clearly demarcating proximal tubules (green) and distal tubules (white) indicated by arrows; weak CL-11 staining (red) is detected in both of these structures. (B) Representative image of ischaemic kidney after 30 min ischaemia and 30 min reperfusion, showing strong staining for CL-11 (red) in the proximal tubules (NCC-negative) and distal (white, NCC-positive) tubules highlighted by the white arrows, and revealing complement deposition (green) only on the proximal tubules. Thus, complement activation is only detected when CL-11 and L-fucose are present together in the proximal tubules. (C) Total numbers (percentages) of either proximal or distal tubules stained positive for C3d from 4 separate fields of ischaemic kidney, showing predominance of C3d deposition in the proximal tubules. P value is for comparison between C3d-positive proximal tubules and C3d-positive distal tubules. Scale bars, 25 μ m.

C

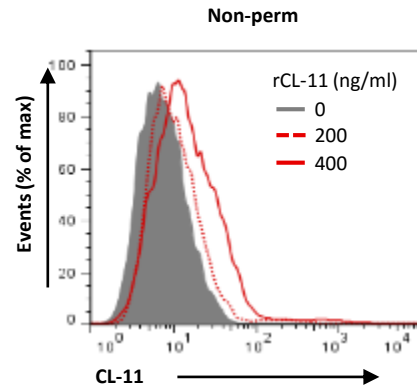
	Proximal tubule (NCC-neg)	Distal tubule (NCC-pos)	P value
C3d-pos	127 (94%)	6 (20%)	< 0.001
C3d-neg	8 (6%)	24 (80%)	
	135 (100%)	30 (100%)	

sFigure 7: Human proximal tubular epithelial cells and detection of endogenous CL-11 and binding of exogenous CL-11

A

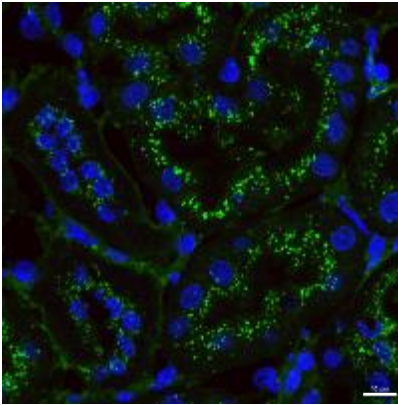


B



Flow cytometry with human proximal tubule epithelial cell line (hPTEC) showing (a) expression of endogenous CL-11 in fixed/permeabilised and (b) binding of added rCL-11 to fixed/non-permeabilised cells in a dose-dependent manner

sFigure 8: Mannose is mainly detected on the apical surface of renal tubular epithelial cells



Fluorescence microscopy of normal (*CL-11^{+/+}*) mouse kidney tissue after staining with fluorescein-labelled galanthus nivalis lectin (GNL), which preferentially detects structures containing (α -1,3) mannose residues. Mannose (green) is detected at the apical but not basolateral surface of renal tubular epithelial cells. Nuclei are stained with DAPI (blue). Scale bar 10 μ m.